PLOS Genetics

Replicative Senescence is Associated with Nuclear Reorganization and with DNA Methylation at Specific Transcription Factor Binding Sites.

--Manuscript Draft--

Manuscript Number:	
Full Title:	Replicative Senescence is Associated with Nuclear Reorganization and with DNA Methylation at Specific Transcription Factor Binding Sites.
Short Title:	DNA Methylation Changes in Replicative Senescence
Article Type:	Research Article
Section/Category:	Epigenetics
Keywords:	senescence; long-term culture; telomere; epigenetic; DNA-methylation; transcription factor binding sites; lamin; massively parallel sequencing
Corresponding Author:	Wolfgang Wagner, M.D., Ph.D. RWTH Aachen University Medical School Aachen, GERMANY
Corresponding Author Secondary Information:	
Corresponding Author's Institution:	RWTH Aachen University Medical School
Corresponding Author's Secondary Institution:	
First Author:	Sonja Hänzelmann
First Author Secondary Information:	
Order of Authors:	Sonja Hänzelmann
	Fabian Beier
	Eduardo G Gusmao
	Carmen M Koch
	Sebastian Hummel
	Iryna Charapitsa
	Sylvia Joussen
	Vladimir Benes
	Tim H Brümmendorf
	George Reid
	Ivan G Costa
	Wolfgang Wagner, M.D., Ph.D.
Order of Authors Secondary Information:	
Abstract:	Primary cells enter replicative senescence after a limited number of cell divisions. This process is associated with reproducible changes in DNA methylation (DNAm) at specific sites in the genome. The mechanism that drives senescence-associated DNAm changes remains unknown - it may involve stochastic DNAm drift due to imperfect maintenance of epigenetic marks, or it is directly regulated at specific sites in the genome. In this study, we analyzed the reorganization of nuclear architecture and DNAm changes during long-term culture of human fibroblasts and mesenchymal stromal cells (MSCs). We demonstrate that telomeres shorten and shift towards the nuclear center at later passages. Concomitantly, DNAm profiles, either analyzed by MethylCap-seq or by 450k Illumina BeadChip technology, revealed consistent senescence-associated hypermethylation in regions associated with H3K27me3

	histone marks, whereas hypomethylation was associated with chromatin containing H3K9me3 and lamina-associated domains (LADs). DNA hypermethylation was significantly enriched in the vicinity of genes that are either up- or down-regulated at later passages. Thus, particularly senescence-associated DNA hypermethylation appears to occur at specific sites in the genome and reflects functional changes in the course of replicative senescence. Furthermore, specific transcription factor binding motifs (e.g. EGR1, TFAP2A, and ETS1) were significantly enriched in differentially methylated regions and in the promoters of differentially expressed genes. These results indicate that tightly regulated epigenetic modifications during long-term culture contribute to changes in nuclear organization and gene expression.
Suggested Reviewers:	Argyris Papantonis, PhD Group Leader, University of Cologne argyris.papantonis@uni-koeln.de Expert in bioinformatics and this type of research
	Phillipe Collas, PhD Professor, Institute of Basic Medical Sciences philippe.collas@medisin.uio.no published relevant work in the field. Expert for this kind of Research.
	Günter Lepperdinger, PhD Professor, University of Innsbruck guenter.lepperdinger@uibk.ac.at Expert for replicative senescence and functional changes in fibroblasts and MSCs. He is familiar with epigenetics in this context.
	Justin Guinney, PhD Group Leader, Fred hutchinson Cancer Research Center jguinney@gmail.com
Opposed Reviewers:	
Additional Information:	
Question	**Response**
Data Availability PLOS journals require authors to make all data underlying the findings described in their manuscript fully available, without restriction and from the time of publication, with only rare exceptions to address legal and ethical concerns (see the PLOS Data Policy and FAQ for further details). When submitting a manuscript, authors must provide a Data Availability Statement that describes where the data underlying their manuscript can be found. Your answers to the following constitute your statement about data availability and will be included with the article in the event of publication. **Please note that simply stating 'data available on request from the author' is not acceptable.** ***If, however, your data are only available upon request from the author(s), you must answer "No" to the first question below, and explain your exceptional situation in the text box provided.*** Do the authors confirm that all data underlying the findings described in their manuscript are fully available without restriction?	Yes - all data are fully available without restriction

Please describe where your data may be found, writing in full sentences. **Your answers should be entered into the box below and will be published in the form you provide them, if your manuscript is accepted.** If you are copying our sample text below, please ensure you replace any instances of XXX with the appropriate details. If your data are all contained within the paper and/or Supporting Information files, please state this in your answer below. For example, “All relevant data are within the paper and its Supporting Information files.” If your data are held or will be held in a public repository, include URLs, accession numbers or DOIs. For example, “All XXX files are available from the XXX database (accession number(s) XXX, XXX)." If this information will only be available after acceptance, please indicate this by ticking the box below. If neither of these applies but you are able to provide details of access elsewhere, with or without limitations, please do so in the box below. For example: “Data are available from the XXX Institutional Data Access / Ethics Committee for researchers who meet the criteria for access to confidential data.” “Data are from the XXX study whose authors may be contacted at XXX.” * typeset	All MethylCap-seq data and RNA-seq data have been deposited at GEO.
Additional data availability information:	

Aachen University Medical School
RWTH AACHEN
Institute for Biomedical Engineering
-Cell Biology-

Wolfgang Wagner, MD, PhD, Univ.-Prof.
Helmholtz Institute for
Biomedical Engineering
Pauwelsstrasse 20
52074 Aachen
Germany

Tel.: +49-241-80 88611
Email: wwagner@ukaachen.de

Prof. Dr. Gregory S. Barsh
Prof. Dr. Gregory P. Copenhaver
Editors in Chief, *PLoS Genetics*

July 29th 2014

Dear Editors of *PLoS Genetics*,

Please find enclosed our manuscript “Replicative senescence is associated with nuclear reorganization and with DNA methylation at specific transcription factor binding sites “, which we would like to submit to *PLoS Genetics* for publication.

Cells undergo dramatic changes during culture expansion until they ultimately reach replicative senescence. Such functional changes need to be taken into account and they are of major relevance in cellular therapy. However, the underlying mechanism is still largely unknown. In this study, we describe that culture expansion is associated with:

1) Changes in nuclear morphology and shift of telomeres towards the nuclear center.
2) DNA methylation (DNAm) profiles of fibroblasts at early and late passages were analyzed by MethylCap-seq. The results were correlated with our previously published data on replicative senescence on 450k Illumina BeadChips (Koch et al., *Genome Res.* 2013).
3) Both of these DNAm datasets revealed consistent senescence-associated hypomethylation in genomic regions associated with H3K9me3 marks and lamina-associated domains (LADs).
4) In contrast, hypermethylation is observed in genes, which are differentially expressed (RNA-Seq data).
5) Genomic regions with senescence-associated DNAm changes and promoter regions of differentially expressed genes reveal highly significant enrichment of similar transcription factor binding motifs.

These results support the notion that epigenetic changes in cellular aging reflect a tightly regulated and functionally relevant process. We believe that these findings will be of interest for a broad readership with interest in cell biology and regenerative medicine. We are looking forward to your opinion.

With best regards,

Ivan Costa and Wolfgang Wagner

Replicative Senescence is Associated with Nuclear Reorganization and with DNA Methylation at Specific Transcription Factor Binding Sites.

Sonja Hänzelmann[1,2], Fabian Beier[3], Eduardo G. Gusmao[1,2], Carmen M. Koch[2,4], Sebastian Hummel[3], Iryna Charapitsa[5], Sylvia Joussen[2,4], Vladimir Benes[6], Tim H. Brümmendorf[3], George Reid[5], Ivan G. Costa[1,2,*], and Wolfgang Wagner[2,4,*]

1. Interdisciplinary Centre for Clinical Research (IZKF), RWTH University Medical School, Aachen, Germany
2. Institute for Biomedical Technology – Cell Biology, RWTH University Medical School, Aachen, Germany
3. Department of Hematology, Oncology, Hemostaseology and Stem Cell Transplantation, RWTH Aachen University Medical School, Aachen, Germany
4. Helmholtz-Institute for Biomedical Engineering, Stem Cell Biology and Cellular Engineering, RWTH University Medical School, Aachen, Germany
5. Institute for Molecular Biology, Mainz, Germany
6. Genomics Core Facility, European Molecular Biology Laboratory (EMBL), Heidelberg, Germany

Running Title: DNA Methylation Changes in Replicative Senescence

Keywords: senescence; long-term culture; telomere; epigenetic; DNA-methylation; transcription factor binding sites; lamin; massively parallel sequencing

*Correspondence: Ivan Costa, PhD; Interdisciplinary Centre for Clinical Research (IZKF), RWTH University Medical School,Pauwelstr 19, 52074 Aachen, Germany; Phone: +49 241 80 80270; Email: ivan.costa@rwth-aachen.de; and Wolfgang Wagner, MD, PhD; Helmholtz-Institute for Biomedical Engineering; RWTH Aachen University Medical School; Pauwelsstrasse 20; 52074 Aachen; Phone: +49 241 8088611; Email: wwagner@ukaachen.de

Abstract

Primary cells enter replicative senescence after a limited number of cell divisions. This process is associated with reproducible changes in DNA methylation (DNAm) at specific sites in the genome. The mechanism that drives senescence-associated DNAm changes remains unknown – it may involve stochastic DNAm drift due to imperfect maintenance of epigenetic marks, or it is directly regulated at specific sites in the genome. In this study, we analyzed the reorganization of nuclear architecture and DNAm changes during long-term culture of human fibroblasts and mesenchymal stromal cells (MSCs). We demonstrate that telomeres shorten and shift towards the nuclear center at later passages. Concomitantly, DNAm profiles, either analyzed by MethylCap-seq or by 450k Illumina BeadChip technology, revealed consistent senescence-associated hypermethylation in regions associated with H3K27me3 histone marks, whereas hypomethylation was associated with chromatin containing H3K9me3 and lamina-associated domains (LADs). DNA hypermethylation was significantly enriched in the vicinity of genes that are either up- or down-regulated at later passages. Thus, particularly senescence-associated DNA hypermethylation appears to occur at specific sites in the genome and reflects functional changes in the course of replicative senescence. Furthermore, specific transcription factor binding motifs (e.g. EGR1, TFAP2A, and ETS1) were significantly enriched in differentially methylated regions and in the promoters of differentially expressed genes. These results indicate that tightly regulated epigenetic modifications during long-term culture contribute to changes in nuclear organization and gene expression.

Author Summary

Cells undergo continuous changes during *in vitro* culture until they ultimately stop proliferation after a limited number of cell divisions - a phenomenon commonly referred to as replicative senescence. It is generally assumed that this process is triggered by accumulation of random cellular defects, such as double strand breaks and telomere attrition. It has also been demonstrated that cellular aging is associated with highly reproducible epigenetic modifications that may reflect a tightly regulated underlying process. In this study, we used different techniques for genome wide comparison of DNA methylation profiles of cells at early and late passages. Overall, loss of DNA methylation is particularly observed in chromatin that is associated with the nuclear envelope. We demonstrate that DNA hypermethylation occurs particularly at genomic regions with binding motifs for specific transcription factors. Conversely, differentially expressed genes also comprised these transcription factor binding sites in their promoter regions. These results provide a link between gain of DNA methylation at specific sites in the genome and senescence-associated gene expression changes. Particularly site-specific hypermethylation seems to be relevant for functional changes of cells during *in vitro* culture.

Introduction

Primary cells lose proliferative potential during *in vitro* culture and enter a senescent state after a limited number of cell divisions [1]. For example fibroblasts and mesenchymal stromal cells (MSCs) undergo continuous morphologic and functional changes in the course of culture expansion. These include an increase in cell size and loss of *in vitro* differentiation potential [2,3]. It is therefore important to define the state of cellular aging in cell preparations and to better understand the mechanisms that elicit these dramatic changes during *in vitro* culture.

The reduction in telomere length has a definitive role in the loss of chromosomal integrity during culture expansion [4,5]. Nuclei of senescent cells reveal further structural changes, such as the development of senescence-associated heterochromatin foci (SAHF) [6], the formation of γH2AX-foci associated with DNA damage and double strand breaks [7], and distorted organization of nuclear lamina [8]. Chromosomes are not randomly organized within the nucleus, but have a preferred position in relation to specific neighboring chromosomes [9,10]. Reorganization of chromosomal territories has been associated with changes in the epigenetic regulation of gene expression [11] and consequently may also be implicated in functional changes resulting from long-term culture of primary cells.

Recent evidence suggests that replicative senescence is accompanied by epigenetic modifications at specific CpG sites [12–14]. These senescence-associated DNA methylation (SA-DNAm) changes are very similar in both fibroblasts and MSCs [14,15], which may result from both cell types being closely related [16]. It has been suggested that long-term culture *in vitro* is associated with global DNA hypomethylation, whereas local DNA hypermethylation occurs at specific CpG sites [17]. SA-DNAm changes are related to, but not identical with age-associated DNAm changes [12,15]. SA-DNAm changes as well as age-associated DNAm changes are enriched in developmental genes, such as homeobox genes [12], coincide with polycomb group target genes [18,19] and with specific histone

marks [13,20]. However, it is unclear how these changes in DNAm patterns are governed and if they are functionally relevant.

Two non-exclusive mechanisms might influence SA-DNAm changes: 1) compatible with the perception of epigenetic drift [21,22], they might result from loss of control at circumscribed genomic regions or 2) DNAm changes are directly controlled by regulated protein complexes (e.g. DNA-methyltransferases) targeting specific regions in the genome. In this study, we characterized nuclear changes during long-term culture of human fibroblasts and MSCs with particular focus on changes in nuclear morphology, telomere distribution, DNAm and gene expression changes to gain further insight in the underlying processes of senescence.

Results

Telomeres shift to the nuclear center during expansion in culture

Nuclei and telomeres were analyzed in human dermal fibroblasts at early (P3 to P5) and corresponding late passages (P21 to P40) with regard to nuclear area and by quantitative fluorescent *in situ* hybridization (Q-Fish) with telomere repeat probes (Figure 1A,B). Overall, nuclear size increased significantly during culture expansion ($p < 0.0001$; t-test; Figure 1C), whereas the thickness remained relatively constant (5 – 7 µm in z-stacks). Furthermore, nuclei acquired an elongated morphology (Figure 1D). As anticipated, telomere length decreased at later passages ($p < 0.0001$; Figure 1E). Localization of telomeres within the nucleus was segmented into either the peripheral region, middle region, or central region [23]. In early passages, telomeres were predominately localized at border regions close to the nuclear lamina while they appeared to be redistributed to the nuclear center at later passages (Figure 1F). Changes in nuclear size, morphology and localization of telomeres reflect chromosomal reorganization during *in vitro* culture expansion.

Analysis of senescence-associated DNA methylation

DNA methylation patterns were measured in two fibroblast preparations at early (P3 or P5) and late passage (P30 or P33). To this end, we used MethylCap-seq, which is based on capturing methylated DNA with the methyl-CpG-binding domain (MBD) of the methyl-CpG-binding protein 2 (MeCP2) and subsequent next-generation sequencing of salt eluted DNA [24]. This analysis revealed that differentially methylated regions (DMRs) occur during culture expansion: 4,309 and 2,864 regions became hypermethylated and 6,489 and 3,613 regions hypomethylated during culture expansion of donor 1 and donor 2 cells, respectively (Figure 2A,B). Regions within the *HOXC* locus revealed prominent DMRs, particularly in donor 2 (Figure 2C). However, the overlap of DMRs between the two donors was only 3.99% and 4.24% for hyper- and hypomethylated regions, respectively. This was in contrast to highly reproducible changes observed during long-term culture of fibroblasts and MSCs when using either IlluminaBeadChip Technology [12,14,19] or whole-genome single-nucleotide bisulfite sequencing [17].

Therefore, we compared the results from MethylCap-seq with our recent study on senescence-associated (SA-) DNAm changes in MSCs using 450k IlluminaBeadChips [19]. With IlluminaBeadChips, 1,702 CpGs were found to be significantly hypomethylated upon long-term culture and 2,116 CpGs became hypermethylated (adjusted P-value < 0.05 and DNAm change > 20%). MethylCap-seq signals were then analyzed in a 600 bp window around these SA-DNAm changes identified by BeadChip technology. Overall, differential MethylCap-seq signals had the same tendency of SA-DNAm changes as observed with the 450k IlluminaBeadChip data (Figure 2D,E). This finding confirmed that consistent senescence-associated DNAm changes occur between IlluminaBeadChip technology and MethylCap-seq– even though the latter revealed less overlap of specific DMRs in biological replicates.

Consequently, we analyzed whether SA-DNAm changes were restricted to individual CpGs or if adjacent CpGs were also affected. We focused on the most significant CpGs of the 450k

IlluminaBeadChip data (1,702 and 2,116 CpGs) and found that SA-hypermethylation and hypomethylation was not restricted to individual CpGs but also occurred in upstream and downstream CpGs, usually within a region of 500 base pairs (Figure 2F,G). There were fluctuations in mean DNAm level of CpGs in the vicinity of CpGs with the most significant SA-DNAm changes which cannot be resolved by analysis of DNA fragments in MethylCap-seq. Therefore, analysis of DNAm at single nucleotide resolution using IlluminaBeadChip technology or genome-wide bisulphite sequencing might be advantageous for analysis of site-specific changes during culture expansion.

Senescence-associated DNAm coincides with histone marks and lamina-associated domains

We then compared DNAm changes resulting from long-term culture with previously published datasets on post-translational histone modifications [25] and on lamina-associated domains (LADs) [26] in human fibroblasts (Figure 3A). Genomic regions with SA-hypermethylation in late-passage samples from fibroblast donor 2 and MSCs revealed significant enrichment in regions with trimethylation on histone 3 at lysine 27 (H3K27me3) (Figure 3B). H3K27me3 is characteristic for inactivated chromatin within gene rich regions [27]. In contrast, H3K9me3, a repressive histone mark mainly occurring in gene poor regions, was associated with non-methylated regions. All samples analyzed had a significant presence of SA-hypomethylation in genomic regions with H3K9me3 marks (Figure 3C). Thus, specific histone modifications are enriched in regions with DNAm changes during long-term culture.

Subsequently, we compared our DNAm datasets with a high-resolution map of genomic interaction sites with the nuclear lamina in human fibroblasts, which comprises 1,239 genomic regions representing about 40% of the human genome [26]. DNAm levels were lower in lamina associated regions than in the remaining genomic regions (Figure 3D). Conversely, H3K27me3 marks were particularly observed outside of LADs, whereas H3K9me3 marks were more prevalent inside LADs as described before [26]. Particularly, LAD borders clearly demarcate the level of DNAm (Figure 3E). We correlated senescence-associated DMRs with LADs and found that hypomethylated sites were

enriched inside LADs while hypermethylated sites were enriched outside of LADs. Similar results were observed with SA-DNAm changes in MSCs, which were determined by 450k BeadChip technology (Figure 3F). We therefore postulated that a shift of lamina-association, particularly at the border regions of LADs, may contribute to DNAm changes during culture expansion. However, the SA-DNAm changes were not related to the borders of LADs. In summary, loss of DNAm during culture expansion is particularly observed in heterochromatin associated with the nuclear lamina, whereas DNA hypermethylation was observed in regions not associated with the lamina.

Gene expression changes during replicative senescence

To further correlate DNAm changes with gene expression changes we sequenced the transcriptome of three MSC preparations at early (P3) and late passage (P13; the same MSC preparations previously used for analysis of DNAm profiles [19]). 648 genes were down-regulated and 499 genes up-regulated during long-term culture (FDR < 0.01 and log2 fold change > 2; Figure 4A; supplemental table 1). Interestingly, amongst the significantly down-regulated genes were lamin B1 (*LMNB1;* $p = 5.9*10^{-13}$) and lamin B2 (*LMNB2*; $p = 4.1*10^{-37}$). Further, down-regulated genes included the lamin B receptor (*LBR*; $p = 6.8*10^{-4}$), which anchors the lamina and heterochromatin to the membrane; thymopoietin (*TMPO*; $p = 3.8*10^{-18}$), which may play a role in the assembly of the nuclear lamina, and thus help maintain the structural organization of the nuclear envelope, and spectrin repeat containing nuclear envelope 2 (*SYNE2*, p = 0.005), whereas *SYNE1* was up-regulated ($p = 3.1*10^{-18}$). These results indicate that differential expression of genes involved in the nuclear lamina may contribute to reorganization of chromatin during long-term culture.

Subsequently, we analyzed whether genes localized within the LADs are particularly affected by senescence. Overall, these genes were less expressed and this was especially observed at the border of LADs (Figure 4B), which is in agreement with previous findings [26]. However, gene expression changes during culture expansion were not related to LADs or to the border of LADs (Figure 4C). The number of up-regulated and down-regulated genes was similar between LADs and non-lamina-

associated regions (Figure 4D). Thus, neither the hypomethylation in LADs nor gene expression changes during culture expansion seem to be triggered by extension or restriction of chromatin interaction sites with the nuclear lamina.

Subsequently, we performed Gene Ontology (GO) analysis of differentially expressed genes to gain better insight in the functional changes during long-term culture: down-regulated genes revealed a highly significant enrichment in categories involved in cell division and DNA repair whereas up-regulated genes were enriched in cell adhesion, development, and extracellular matrix organization (Figure 4E). This is in line with our previous reports using microarray analysis of RNA profiles in culture expansion [2]. We compared changes in the DNAm pattern upon culture expansion with differential gene expression. Overall, hypermethylated regions were enriched in the vicinity of up-regulated and down-regulated genes, while hypomethylated regions were neither enriched in the vicinity of neither up-regulated nor down-regulated genes (Table 1). These findings suggest that hypermethylation of specific genomic regions impacts on gene expression changes during culture expansion.

Transcription factor binding sites in senescence-associated DMRs

Next, we performed a transcription factor (TF) binding site analysis in regions with SA-DNAm changes (450k BeadChip and MethylCap-seq data): 51 motifs were significantly enriched (p-value < 0.05; Fisher's Exact test) in senescence-associated DMRs of at least one fibroblast sample or of MSCs. Most of these TF binding motifs were significantly enriched in both hypermethylated and hypomethylated regions (Figure 5A). Significantly over-represented motifs include binding sites for early growth response protein 1 (EGR1), activating enhancer-binding protein 2 (TFAP2A), protein C-ets-1 (ETS1), neuroblastoma MYC oncogene (MYCN), and aryl hydrocarbon receptor (ARNT; Figure 5B). Enrichment of these TF binding sites suggests that they are either directly involved in the regulation of SA-DNAm changes or that their binding is influenced by differential methylation and hence relevant for gene expression changes.

Therefore, we analyzed enrichment of TF binding sites in the promoter regions (1kb upstream) of the differentially expressed genes: 64 motifs were enriched and most of these were enriched in promoter regions of both up- and down-regulated genes (Figure 5C). There is a highly significant overlap of TF motifs enriched in DMRs and differentially expressed genes upon long-term culture (22 motifs marked in bold in Figure 5A and 5C; p-value < 10^{-4}; Fisher's Exact test). This enrichment of specific TF binding sites indicates that corresponding factors are relevant for the functional changes during long-term culture.

Discussion

In this study we demonstrate various facets of the impact replicative senescence has on nuclear organization (Figure 6). This complex picture suggests that different mechanisms are involved in senescence-associated changes, with hypomethylation enriched in inactivated LADs, whereas hypermethylation is reflected by specific changes in gene expression.

Telomere length is well known to decline before cells enter replicative senescence. However, the intranuclear positioning of telomeres, which again reflects a major change in genomic organization, is less clear. It has recently been demonstrated that telomeres are enriched at the nuclear periphery during postmitotic nuclear assembly and become localized at the nuclear center during cell cycle arrest [23]. We also find that telomeres shift away from the nuclear envelope towards the nuclear center at later passages. Transient proximity of telomeres to the nuclear envelope, as well as interaction with A-type lamins, has been suggested to support telomere maintenance, particularly at early passage [28]. In senescent cells, distortion of the ellipsoid-like nuclear shape and lamin A folds protruding into the nucleoplasm have been described [29], which may also contribute to redistribution of telomeres in senescent cells. Such changes in nuclear organization may also entail alterations in the epigenetic make up during cell senescence – or *vice versa*.

The DNAm pattern changes during culture expansion in a highly reproducible manner. In fact, an Epigenetic-Senescence-Signature based on DNAm at six specific CpGs even facilitates reliable prediction of passage numbers and cumulative population doublings for quality control of cell preparations [14,30,31]. So far, DNAm changes in replicative senescence were observed in datasets either based on IlluminaBeadChip technology or pyrosequencing of bisulfite converted DNA. In this regard, it was unexpected that the MethylCap-seq data had relatively little overlap between DNAm changes in the two different fibroblast preparations. MethylCap-seq is a robust method for genome-wide DNAm profiling [24,32]. However, reproducibility of specific DNAm changes during culture expansion may be hampered for various reasons: there are notoriously inter-individual differences and variation between cell types, deviations in DNA fragmentation. and efficiency of pull down. Furthermore, results in MethylCap-seq are influenced by various parameters in bioinformatic pipelines used for detection of DMRs. MethylCap-seq does not provide DNAm level at single nucleotide resolution. Although, SA-DNAm changes are not restricted to individual CpGs, we demonstrated that there is reproducible fluctuation of DNAm in their vicinity, possibly due to a local action of DNA binding proteins. Furthermore, age-associated DNAm changes, which are highly reproducible when using the IlluminaBeadChip platform [21,33,34] revealed much lower reproducibility in MethylCap-seq data [35]. Therefore, methods which address DNAm at single site resolution - such as pyrosequencing, MassArray, microarray technology, or whole genome bisulphite sequencing - seem to be advantageous in tracking specific senescence-associated CpGs. On the other hand, our results based on MethylCap-seq data further validate changes in the DNAm pattern during culture expansion using a different approach, which does not require bisulfite conversion.

We have previously suggested that senescence-associated DNAm changes are related to specific histone modifications by characterizing the promoter regions of genes with SA-CpGs [13]. Further, age-associated hypermethylation is enriched in genes of polycomb group targets, defined by high occupancy of SUZ12, EED and H3K27me3 in mice [36] and in human [18,33,34,37]. In this study, we

specifically analyzed H3K27me3 and H3K9me3 profiles at the genomic location of DMRs. There is a moderate enrichment of SA-hypermethylation with H3K27me3 marks in fibroblasts. We have observed an opposite tendency in our previous work [19]. However, the latter analysis was based on H3K27me3 around the promoter of genes close to SA-hypermethylation, while our current analysis is based on the regions around the hypermethylated sites. More interestingly, there was significant enrichment of SA-hypomethylation with H3K9me3 in all datasets analyzed. Association of DNAm changes with the histone code indicates that both mechanisms interact and may even be dependent on each other: either the DNAm pattern affects activity of histone modifiers or changes in heterochromatin evoked by the histone code impact on DNA methylation.

The inner layer of the envelope consists of filamentous proteins: lamin A and C, which are splice variants of the *LMNA* gene, and lamin B1 and lamin B2, encoded by *LMNB1* and *LMNB2*, respectively [38]. Mutations of these genes can affect chromosomal organization [39,40] and such mutations are involved in multiple human diseases such as cardiac and skeletal myopathies [41], and premature aging [11]. *LMNB1* and *LMNB2* were amongst the most significantly down-regulated genes during culture expansion. In fact, it has been demonstrated that loss of *LMNB1* is a biomarker for senescence [42], whereas over expression of LMNB1 increases proliferation and delays onset of senescence in WI-38 cells [43]. Furthermore, it has recently been demonstrated that lamin B1 down-regulation in senescence is a key trigger of global and local chromatin changes [44]. The lamin B receptor (*LBR*) was also significantly down-regulated. LBR interacts with methyl-CpG-binding protein 2 (MeCP2), the same methylation binding domain used to capture methylated DNA for MethylCap-seq. This interaction has been suggested to have a role in the localization and/or stabilization of transcriptionally silent heterochromatin adjacent to the nuclear envelope [45]. LADs are implicated in epigenetic regulation due to their relevance for chromosome positioning and influence on chromatin structure [46]. Therefore, remodeling may activate gene expression by moving genes away from the lamina [47]. We demonstrate that loss of DNAm is particularly observed in LADs and that is in agreement with another recent study using whole-genome single-nucleotide bisulfite sequencing in IMR90 cells of

early and late passage [17]. It may therefore be speculated that heterochromatin, which is tightly linked to LADs, interferes with accessibility of DNMT1 during cell cycle and hence hypomethylation over subsequent passages [17]. This might mechanistically define epigenetic drift during long-term culture.

In contrast, SA-hypermethylation seems to be associated with differential gene expression of both up- and down-regulated genes. These functional changes are reflected by highly specific enrichment of up-regulated genes in categories of cellular organization and development whereas down-regulated genes are involved in cell division. Association of DMRs with differential gene expression, even though not necessarily negatively correlated, implies that the SA-hypermethylation may be relevant for these gene expression changes. In fact, several TFs predicted to bind to DMRs and differentially expressed genes upon senescence have been implicated in replicative senescence before: ERG1, also known as zinc finger protein 225, has been shown to play a central role for aging [48,49] and replicative senescence [50]. It has been suggested that deletion of EGR1 leads to a striking phenotype with complete bypass of senescence and apparent immortalization [50]. ETS1, which belongs to the ETS family of downstream targets of the RAS-RAF-MEK signaling pathway, activates the p16INK4a promoter thereby affecting senescence [51]. N-MYC is a proto-oncogene protein that is known to be involved in regulation of developmental timing in *Caenorhabditis elegans* [52]. Concretely, its binding motif is similar to binding motifs for C-MYC which has also been shown to antagonize senescence and to support reprogramming into the pluripotent state. Also, EGR1, MYCN and ARNT all have a CpG sequence in their core binding motif. It is conceivable that binding of these TFs is relevant for regulation of DMR, potentially by interaction with DNA methyltransferases. However, this is not yet conclusive as hyper- and hypomethylated SA-DNAm changes reveal overlapping enrichment of similar TF-binding motifs. Alternatively, SA-DNAm changes play a role to modulate binding of relevant TFs, particularly in hypermethylated regions that coincide with differentially expressed genes.

Conclusion

In this study, we provide evidence that epigenetic changes during long-term culture reflect changes in nuclear organization. It remains unclear whether SA-DNAm alterations are due to epigenetic drift or to a tightly regulated process with the possibility that both mechanisms are involved in this process. The finding that SA-hypomethylation is enriched in LADs and H3K9me3 marks without association to specific gene expression changes is compatible with passive and stochastic changes in DNAm level. In contrast, specific SA-hypermethylation is reflected in differential gene expression. Furthermore, the association of SA-DNAm changes with TF-binding sites indicates a functionally relevant and controlled process. Notably, both SA-hypermethylation and SA-hypomethylation are reversed when reprogrammed into iPSCs, which may reflect rejuvenation also on the epigenetic level [19]. In this regard, senescence-associated epigenetic modifications seem to be controlled at specific sites in the genome - either actively or passively - and entail the functional changes in the course of replicative senescence.

Materials and Methods

Isolation of primary cells

Human dermal fibroblasts were isolated from patients undergoing surgical interventions after written consent, using guidelines approved by the Ethic Committee on the Use of Human Subjects at the University of Aachen (Permit Number EK163/07) as described in detail before [15]. Cells were culture expanded in DMEM culture medium (PAA; 1g/L glucose) supplemented with glutamine (PAA), penicillin/streptomycin (PAA), and 10% fetal calf serum (FCS; Biochrom, Berlin, Germany) in a humidified atmosphere at 5% CO_2. Cells were culture expanded until replicative senescence as determined by ultimate growth arrest. Late passages (as indicated in the text) were within the last three to five passages before entering senescence.

Mesenchymal stromal cells were isolated from the bone marrow of caput femoris upon hip replacement surgery after written consent using guidelines approved by the Ethic Committee on the Use of Human Subjects at the University of Aachen (Permit Number EK128/09) as described before [19]. MSCs were culture expanded in DMEM culture medium (PAA) with supplemented with glutamine (PAA), penicillin/streptomycin (PAA), and 10% human platelet lysate (hPL) [53] in a humidified atmosphere at 5% CO_2. All cell preparations were characterized with regard to immunophenotype and *in vitro* differentiation potential towards osteogenic and adipogenic lineages as described before [15,19].

Q-FISH analysis of telomeres

Quantitative fluorescent *in situ* hybridization (Q-FISH) was performed on cytospins of three fibroblast preparations of early (P3-5) and corresponding late passages (P 21-40). Staining with a telomere probe labeled with Cy3 (Panagene, Daejeon, Korea) and counterstaining with DAPI was performed as described previously [54,55]. Cells sections were captured in multi-tracking mode (1 µm step size) using a high-resolution Zeiss confocal microscope (LSM710, Zeiss, Jena, Germany). At least 25 nuclei were captured per cell preparation. Definiens XD 2.0 software (Definiens GmbH, Germany) was used for image analysis. Telomere length was calculated by the mean telomere spot intensity with mean background subtraction of the respective nucleus on maximum projection images. To calculate the distance of the detected telomeres in relation to the nucleus, the single z-stack image with the largest nuclei area was analyzed. Nuclei were defined in three different zones as recently described [23]. Three zones in the nucleus were defined: Border, middle and center zone. Nuclear size was normalized (absolute pixel distances) allowing comparison in different nuclei. At least three telomeres had to be detected in one nucleus to be included in the analysis.

DNA methylation analysis

DNA methylation profiles were analyzed by methyl-capture sequencing (MethylCap-seq), which is based on precipitation of methylated DNA by recombinant methyl-CpG binding domain of MeCP2

protein. Fibroblasts from two female donors (both 43 years old) were expanded in culture and DNA from 10^7 cells was harvested from cells at early passage (P3 or P5) and late passage (P30 and P33) using the Qiagen DNA Blood Midi-Kit. DNA quality was assessed with a NanoDrop ND-1000 spectrometer (NanoDrop Technologies, Wilmigton, USA) and gel electrophoresis. DNA was sheared with an S220 focused-ultrasonicator (Covaris Inc., Woburn, USA)to a size range of 200-400 bp and then incubated with 2 µg of recombinant MBD2-glutathion-S-transferase fusion protein with a histidine tag(H6) [24]. Methylated DNA fragments were then captured on NTA-agarose magnetic bead s(Sigma, H9914) and following washing, eluted by 0.4 M NaCl. Library preparation of methylated DNA fragments and deep sequencing with Illumina technology (IlluminaInc., San Diego, USA) with a read length of 36 bases was performed at EMBL gene core facility (Heidelberg, Germany). Data have been deposited at NCBIs Gene Expression Omnibus (GEO, http://www.ncbi.nlm.nih.gov/geo/). In addition, we used our previously published DNAm profiles of MSCs during long-term culture (GSE37066)[19].

RNA sequencing

RNA was isolated from 10^6 cells of three MSC donors (59, 64, and 73 years old) at passage 4 and passage 13 using the miRNeasy Mini Kit (Qiagen). Quality control and measurement of RNA concentration was done with a NanoDrop Spectrophotometer (Thermo Scientific, Wilmington, USA) and the Agilent 2100 Bioanalyzer (Agilent Technologies). Multiplexed library preparation of total RNA and deep sequencing with IlluminaHiSeq 2000 technology (IlluminaInc., San Diego, USA) with a read length of 50 bases was performed at EMBL gene core facility (Heidelberg, Germany). RNA-Seq profiles have been deposited at GEO.

Bioinformatic analysis

Methylcap-seq and RNA-Seq data was subjected to quality control check and preprocessing steps using fastQC (http://www.bioinformatics.babraham.ac.uk/projects/fastqc/) and Flexbar [56]. In all figures, MethylCap, Chip-Seq, and RNA signals were normalized to obtain reads per kilobase millions

(RPKM) to correct the signal intensities when comparing multiple signals derived from sequencing methods.

For Methylcap-Seq, alignment to the human genome built 37 (hg19) was done with Burrows-Wheeler Transform (BWA) [57]. More than 20 million reads per sample were mapped to the genome. We calculated differentially methylated regions for each donor individually by comparing early passage *versus* corresponding late passage. DMR detection was performed with model-based analysis of ChIP-Seq (MACS; default parameters) [58]. For obtaining hypermethylated regions we supplied late passage as signal and early passage as a control signal. The opposite was performed to obtain hypomethylated regions. We complemented the analysis with H3K27me3 and H3K9me3 data (aligned reads) from foreskin fibroblasts from the Epigenomics Roadmap project [25].

The RNA-Seq reads were mapped to the human genome (hg 19) using Bowtie2 [59] and Tophat2 [60]. We used HTSeq [61] with Ensemble 37 (release 71) annotation for quantification of transcripts. Normalization and differential expression analysis were done with DESeq2 [62]. We chose an FDR of 0.01 and a log2 fold change of 2 to detect differentially expressed genes in early or late passage. We used the projection test from the GenometriCorr Package [63] to find associations between DMR signatures and differentially expressed genes.

Regulatory Genomics Analysis

Transcription factor enrichment analysis was performed with the Regulatory Genomics Toolbox (www.regulatory-genomics.org). Regarding DMRs, we extended or shortened the regions to have a length of 40 bps. For up-/down-regulated genes, we used 1kb regions upstream of the transcription start sites as promoter regions (Ensemble 37, release 71). Next, we performed motif match analysis with a false discovery rate (FDR) of 0.0001 [64]. Motifs were obtained in Jaspar and Uniprobe databases [65–67]. The same procedure was repeated 100 times on random genomic regions with same size of the genomic regions tested. We employed a one-tailed Fisher's Exact test to measure

whether the proportion of binding sites of a motif inside the regions is higher than the proportion of binding sites in random regions. Final *p*-values were corrected by the Benjamini-Hochberg method [68].

Acknowledgments

This work was supported by the Stem Cell Network of the state North Rhine Westphalia, by the German Research Foundation (DFG; WA 1706/2-1), by the German Ministry of Education and Research (BMBF; OBELICS) and by the Interdisciplinary Center for Clinical Research (IZKF) within the faculty of Medicine at the RWTH Aachen University. RWTH Aachen University Medical School has applied for patent applications for the Epigenetic-Senescence-Signature and Wolfgang Wagner is involved in the company Cygenia, which provides service for this method to other researchers (www.cygenia.com). Apart from this, the authors have nothing to disclose.

Author Contributions

Conceived and designed experiments: SHä FB CMC WW; performed the experiments: CMK SHu IC SJ GR; analyzed the data: SHä FB EGG GR IGC; contributed analysis tools: VB THB; contributed to writing of the manuscript: SHä GR IGC WW.

References

1. Hayflick L (1965) The limited in vitro lifetime of human diploid cell strains. Exp Cell Res 37: 614-636.
2. Wagner W, Horn P, Castoldi M, Diehlmann A, Bork S, et al. (2008) Replicative Senescence of Mesenchymal Stem Cells - a Continuous and Organized Process. PLoS ONE 5: e2213.
3. Schellenberg A, Stiehl T, Horn P, Joussen S, Pallua N, et al. (2012) Population Dynamics of Mesenchymal Stromal Cells during Culture Expansion. Cytotherapy 14: 401-411.
4. Lansdorp PM (2008) Telomeres, stem cells, and hematology. Blood 111: 1759-1766.
5. Drummond MW, Balabanov S, Holyoake TL, Brummendorf TH (2007) Concise review: Telomere biology in normal and leukemic hematopoietic stem cells. Stem Cells 25: 1853-1861.

6. Narita M, Nunez S, Heard E, Narita M, Lin AW, et al. (2003) Rb-mediated heterochromatin formation and silencing of E2F target genes during cellular senescence. Cell 113: 703-716.

7. d'Adda di FF, Reaper PM, Clay-Farrace L, Fiegler H, Carr P, et al. (2003) A DNA damage checkpoint response in telomere-initiated senescence. Nature 426: 194-198.

8. Capell BC, Collins FS (2006) Human laminopathies: nuclei gone genetically awry. Nat Rev Genet 7: 940-952.

9. Fraser P, Bickmore W (2007) Nuclear organization of the genome and the potential for gene regulation. Nature 447: 413-417.

10. Cremer T, Cremer M, Dietzel S, Muller S, Solovei I, et al. (2006) Chromosome territories--a functional nuclear landscape. Curr Opin Cell Biol 18: 307-316.

11. Puckelwartz MJ, Depreux FF, McNally EM (2011) Gene expression, chromosome position and lamin A/C mutations. Nucleus 2: 162-167.

12. Bork S, Pfister S, Witt H, Horn P, Korn B, et al. (2010) DNA Methylation Pattern Changes upon Long-Term Culture and Aging of Human Mesenchymal Stromal Cells. Aging Cell 9: 54-63.

13. Schellenberg A, Lin Q, Schueler H, Koch C, Joussen S, et al. (2011) Replicative senescence of mesenchymal stem cells causes DNA-methylation changes which correlate with repressive histone marks. Aging (Albany NY) 3: 873-888.

14. Koch CM, Joussen S, Schellenberg A, Lin Q, Zenke M, et al. (2012) Monitoring of Cellular Senescence by DNA-Methylation at Specific CpG sites. Aging Cell 11: 366-369.

15. Koch C, Suschek CV, Lin Q, Bork S, Goergens M, et al. (2011) Specific Age-associated DNA Methylation Changes in Human Dermal Fibroblasts. PLoS ONE 6: e16679.

16. Horwitz EM, Le Blanc K., Dominici M, Mueller I, Slaper-Cortenbach I, et al. (2005) Clarification of the nomenclature for MSC: The International Society for Cellular Therapy position statement. Cytotherapy 7: 393-395.

17. Cruickshanks HA, McBryan T, Nelson DM, Vanderkraats ND, Shah PP, et al. (2013) Senescent cells harbour features of the cancer epigenome. Nat Cell Biol 15: 1495-1506.

18. Teschendorff AE, Menon U, Gentry-Maharaj A, Ramus SJ, Weisenberger DJ, et al. (2010) Age-dependent DNA methylation of genes that are suppressed in stem cells is a hallmark of cancer. Genome Res 20: 440-446.

19. Koch CM, Reck K, Shao K, Lin Q, Joussen S, et al. (2013) Pluripotent stem cells escape from senescence-associated DNA methylation changes. Genome Res 23: 248-259.

20. Rakyan VK, Down TA, Maslau S, Andrew T, Yang TP, et al. (2010) Human aging-associated DNA hypermethylation occurs preferentially at bivalent chromatin domains. Genome Res 20: 434-439.

21. Hannum G, Guinney J, Zhao L, Zhang L, Hughes G, et al. (2013) Genome-wide Methylation Profiles Reveal Quantitative Views of Human Aging Rates. Mol Cell 49: 459-367.

22. Teschendorff AE, West J, Beck S (2013) Age-associated epigenetic drift: implications, and a case of epigenetic thrift? Hum Mol Genet 22: 7-15.

23. Crabbe L, Cesare AJ, Kasuboski JM, Fitzpatrick JA, Karlseder J (2012) Human telomeres are tethered to the nuclear envelope during postmitotic nuclear assembly. Cell Rep 2: 1521-1529.

24. Brinkman AB, Simmer F, Ma K, Kaan A, Zhu J, et al. (2010) Whole-genome DNA methylation profiling using MethylCap-seq. Methods 52: 232-236.

25. Bernstein BE, Stamatoyannopoulos JA, Costello JF, Ren B, Milosavljevic A, et al. (2010) The NIH Roadmap Epigenomics Mapping Consortium. Nat Biotechnol 28: 1045-1048.

26. Guelen L, Pagie L, Brasset E, Meuleman W, Faza MB, et al. (2008) Domain organization of human chromosomes revealed by mapping of nuclear lamina interactions. Nature 453: 948-951.

27. Zhu J, Adli M, Zou JY, Verstappen G, Coyne M, et al. (2013) Genome-wide Chromatin State Transitions Associated with Developmental and Environmental Cues. Cell 152: 642-654.

28. Gonzalez-Suarez I, Redwood AB, Perkins SM, Vermolen B, Lichtensztejin D, et al. (2009) Novel roles for A-type lamins in telomere biology and the DNA damage response pathway. EMBO J 28: 2414-2427.

29. Raz V, Vermolen BJ, Garini Y, Onderwater JJ, Mommaas-Kienhuis MA, et al. (2008) The nuclear lamina promotes telomere aggregation and centromere peripheral localization during senescence of human mesenchymal stem cells. J Cell Sci 121: 4018-4028.

30. Koch CM, Wagner W (2013) Epigenetic Biomarker to Determine Replicative Senescence of Cultured Cells. Methods in Molecular Biology 1048: 309-21.

31. Schellenberg A, Mauen S, Koch CM, Jans R, de WP, et al. (2014) Proof of principle: quality control of therapeutic cell preparations using senescence-associated DNA-methylation changes. BMC Res Notes 7: 254.

32. Serre D, Lee BH, Ting AH (2010) MBD-isolated Genome Sequencing provides a high-throughput and comprehensive survey of DNA methylation in the human genome. Nucleic Acids Res 38: 391-399.

33. Weidner CI, Lin Q, Koch CM, Eisele L, Beier F, et al. (2014) Aging of blood can be tracked by DNA methylation changes at just three CpG sites. Genome Biol 15: R24.

34. Horvath S (2013) DNA methylation age of human tissues and cell types. Genome Biol 14: R115.

35. McClay JL, Aberg KA, Clark SL, Nerella S, Kumar G, et al. (2014) A methylome-wide study of aging using massively parallel sequencing of the methyl-CpG-enriched genomic fraction from blood in over 700 subjects. Hum Mol Genet 23: 1175-1185.

36. Maegawa S, Hinkal G, Kim HS, Shen L, Zhang L, et al. (2010) Widespread and tissue specific age-related DNA methylation changes in mice. Genome Res 20: 332-340.

37. Bocker MT, Hellwig I, Breiling A, Eckstein V, Ho AD, et al. (2011) Genome-wide promoter DNA methylation dynamics of human hematopoietic progenitor cells during differentiation and aging. Blood 117: e182-e189.

38. Aebi U, Cohn J, Buhle L, Gerace L (1986) The nuclear lamina is a meshwork of intermediate-type filaments. Nature 323: 560-564.

39. Lund E, Oldenburg AR, Delbarre E, Freberg CT, Duband-Goulet I, et al. (2013) Lamin A/C-promoter interactions specify chromatin state-dependent transcription outcomes. Genome Res 23: 1580-1589.

40. Collas P, Lund EG, Oldenburg AR (2014) Closing the (nuclear) envelope on the genome: how nuclear lamins interact with promoters and modulate gene expression. Bioessays 36: 75-83.

41. Mewborn SK, Puckelwartz MJ, Abuisneineh F, Fahrenbach JP, Zhang Y, et al. (2010) Altered chromosomal positioning, compaction, and gene expression with a lamin A/C gene mutation. PLoS ONE 5: e14342.

42. Freund A, Laberge RM, Demaria M, Campisi J (2012) Lamin B1 loss is a senescence-associated biomarker. Mol Biol Cell 23: 2066-2075.

43. Shimi T, Butin-Israeli V, Adam SA, Hamanaka RB, Goldman AE, et al. (2011) The role of nuclear lamin B1 in cell proliferation and senescence. Genes Dev 25: 2579-2593.

44. Shah PP, Donahue G, Otte GL, Capell BC, Nelson DM, et al. (2013) Lamin B1 depletion in senescent cells triggers large-scale changes in gene expression and the chromatin landscape. Genes Dev 27: 1787-1799.

45. Guarda A, Bolognese F, Bonapace IM, Badaracco G (2009) Interaction between the inner nuclear membrane lamin B receptor and the heterochromatic methyl binding protein, MeCP2. Exp Cell Res 315: 1895-1903.

46. Reddy KL, Zullo JM, Bertolino E, Singh H (2008) Transcriptional repression mediated by repositioning of genes to the nuclear lamina. Nature 452: 243-247.

47. Peric-Hupkes D, Meuleman W, Pagie L, Bruggeman SW, Solovei I, et al. (2010) Molecular maps of the reorganization of genome-nuclear lamina interactions during differentiation. Mol Cell 38: 603-613.

48. Zimmerman SM, Kim SK (2014) The GATA transcription factor/MTA-1 homolog egr-1 promotes longevity and stress resistance in Caenorhabditis elegans. Aging Cell 13: 329-339.

49. Pardo PS, Boriek AM (2012) An autoregulatory loop reverts the mechanosensitive Sirt1 induction by EGR1 in skeletal muscle cells. Aging (Albany NY) 4: 456-461.

50. Krones-Herzig A, Adamson E, Mercola D (2003) Early growth response 1 protein, an upstream gatekeeper of the p53 tumor suppressor, controls replicative senescence. Proc Natl Acad Sci U S A 100: 3233-3238.

51. Ohtani N, Zebedee Z, Huot TJ, Stinson JA, Sugimoto M, et al. (2001) Opposing effects of Ets and Id proteins on p16INK4a expression during cellular senescence. Nature 409: 1067-1070.

52. Keane M, de Magalhaes JP (2013) MYCN/LIN28B/Let-7/HMGA2 pathway implicated by meta-analysis of GWAS in suppression of post-natal proliferation thereby potentially contributing to aging. Mech Ageing Dev 134: 346-348.

53. Lohmann M, Walenda G, Hemeda H, Joussen S, Drescher W, et al. (2012) Donor Age of Human Platelet Lysate Affects Proliferation and Differentiation of Mesenchymal Stem Cells. PLoS ONE

54. Varela E, Schneider RP, Ortega S, Blasco MA (2011) Different telomere-length dynamics at the inner cell mass versus established embryonic stem (ES) cells. Proc Natl Acad Sci U S A 108: 15207-15212.

55. Beier F, Foronda M, Martinez P, Blasco MA (2012) Conditional TRF1 knockout in the hematopoietic compartment leads to bone marrow failure and recapitulates clinical features of dyskeratosis congenita. Blood 120: 2990-3000.

56. Dodt M, Roehr J, Ahmad R, Dieterich C (2012) FLEXBAR-Flexible Barcode and Adapter Processing for Next-Generation Sequencing Platforms. Biology 1: 895-905.

57. Li H, Durbin R (2009) Fast and accurate short read alignment with Burrows-Wheeler transform. Bioinformatics 25: 1754-1760.

58. Zhang Y, Liu T, Meyer CA, Eeckhoute J, Johnson DS, et al. (2008) Model-based analysis of ChIP-Seq (MACS). Genome Biol 9: R137.

59. Langmead B, Salzberg SL (2012) Fast gapped-read alignment with Bowtie 2. Nat Methods 9: 357-359.

60. Kim D, Pertea G, Trapnell C, Pimentel H, Kelley R, et al. (2013) TopHat2: accurate alignment of transcriptomes in the presence of insertions, deletions and gene fusions. Genome Biol 14: R36.

61. Anders S, Pyl PT, Huber W (2014) HTSeq A Python framework to work with high-throughput sequencing data. Biorxiv 1: doi: 10.1101/002824.

62. Love MI, Huber W, Anders S (2014) Moderated estimation of fold change and dispersion for RNA-Seq data with DESeq2. Biorxiv 1: doi: 10.1101/002832.

63. Favorov A, Mularoni L, Cope LM, Medvedeva Y, Mironov AA, et al. (2012) Exploring massive, genome scale datasets with the GenometriCorr package. PLoS Comput Biol 8: e1002529.

64. Wilczynski B, Dojer N, Patelak M, Tiuryn J (2009) Finding evolutionarily conserved cis-regulatory modules with a universal set of motifs. BMC Bioinformatics 10: 82.

65. Newburger DE, Bulyk ML (2009) UniPROBE: an online database of protein binding microarray data on protein-DNA interactions. Nucleic Acids Res 37: D77-D82.

66. Bryne JC, Valen E, Tang MH, Marstrand T, Winther O, et al. (2008) JASPAR, the open access database of transcription factor-binding profiles: new content and tools in the 2008 update. Nucleic Acids Res 36: D102-D106.

67. Matys V, Kel-Margoulis OV, Fricke E, Liebich I, Land S, et al. (2006) TRANSFAC and its module TRANSCompel: transcriptional gene regulation in eukaryotes. Nucleic Acids Res 34: D108-D110.

68. Hochberg Y, Benjamini Y (2009) Controlling the false discovery rate: a practical and powerful approach to multiple testing. Journal of the Royal Statistical Society 57: 289-300.

Tables

Table 1: Association of DMRs and gene expression changes using the projection test.

DNAm	geneexpression	enriched/depleted	p-value
SA-hyperFibro1	down regulated genes	enriched	2.44E-08
SA-hyperFibro2	down regulated genes	enriched	1.88E-05
SA-hyperMSC	down regulated genes	enriched	1.30E-07
SA-hyperFibro1	up regulated genes	enriched	0.011
SA-hyperFibro2	up regulated genes	enriched	2.07E-09
SA-hyperMSC	up regulated genes	enriched	0.006
SA-hypoFibro1	up regulated genes		no significance
SA-hypoFibro2	up regulated genes		no significance
SA-hypoMSC	up regulated genes		no significance
SA-hypoFibro1	down regulated genes	depleted	0.0008
SA-hypoFibro2	down regulated genes		no significance
SA-hypoMSC	down regulated genes		no significance

Figures

Figure 1: Telomere distribution in senescent fibroblasts.

Telomeres were analyzed by Q-Fish (labeled with Cy3) in nuclei of fibroblasts of early or late passage (n = 3). The nuclear region was counterstained with DAPI. An overview of a cytospin **(A)** and enlarged nuclei at early and late passage **(B)** are exemplarily depicted. Separation of nuclear zones in border, middle and center is indicated by yellow, white, and violet lines, respectively (size bar = 5 µm). Overall, the nuclear area was greatly increased in cells of late passage **(C)** and nuclei became more elongated **(D)**.Telomere length markedly decreased in fibroblasts of late passage **(E)** (a.u. = arbitrary units; error bars depict standard error of nuclei analyzed; early passage: 374 nuclei; late passage: 151 nuclei). The distribution of telomeres changed upon senescence: in early passages (purple dots) they were primarily localized in border and middle regions, whereas distribution changed towards the nuclear center in late passages (yellow dots, data from three biological replica, t-test in all statistical analyses) **(F)**.

Figure 2. Senescence-associated DNAm changes.

Scatter plots of global DNAm profiles (analyzed by methyl-capture sequencing) of early *versus* late passage are depicted for fibroblasts of donor 1 **(A)** and 2 **(B)** (DMR = differentially methylated region; log2 signal intensities are depicted for each DMR). Prominent DMRs were observed within the *HOXC* locus **(C)**. Senescence-associated DNAm changes in fibroblasts (MethylCap-seq data) were then compared to DNAm changes upon long-term culture of MSCs (450k IlluminaBeadChip) of our previous work [19]. Differential DNAm levels (late minus early passage) in fibroblast 1 **(D)** and 2 **(E)** were analyzed at genomic regions surrounding the CpGs with senescence-associated DNAm changes in MSCs. This comparison reflected overlap of senescence-associated DNAm changes between the two methods and cell types. Subsequently, we analyzed the mean DNAm level of neighboring CpGs in a 500bp window in the vicinity of CpGs with significant SA-hypermethylation **(F)** and SA-hypomethylation **(G)**.

Figure 3. Senescence-associated hypomethylation is enriched in lamina-associated domains.

DNAm profiles of fibroblasts at early and late passage (MethylCap-seq) were compared to previously published data on H3K27me3 [25], H3K9me3 [25], and lamina associated domains (LADs) [26] in fibroblasts. Non-methylated DNA was particularly associated with the histone mark H3K9me3 and LADs, whereas H3K27me3 was significantly reduced in these regions. RPKM signals are exemplarily depicted for a region in chromosome 16 **(A)**. Distributions of average RPKM levels of H3K27me3 **(B)** and H3K9me3 **(C)** in 1000 bp windows around DMRs are shown. Average signal intensity of DNAm was significantly lower inside LADs than outside LADs (Mann–Whitney test of equal means) **(D)**. A particular sharp decline of DNAm level was observed at the border of LADs – this was observed in all samples **(E)**. Senescence-associated DMRs were then correlated with LADs. The proportion of senescence-associated (SA) hypermethylation was significantly decreased in LADs while SA-hypomethylation was highly significantly increased in LADs as compared to randomly selected regions (two tailed Fisher's Exact test) **(F)**.

Figure 4. Gene expression changes upon long-term culture.

Gene expression profiles (RNA-seq) were analyzed in MSCs of early passage (P4) and late passage (P13; n = 3). The volcano plot demonstrates differential expression upon long-term culture. Relevant genes are indicated in red **(A)**. Particularly, genes localized at the border of LADs were hardly expressed **(B)**. No significant association of senescence-associated gene expression changes was observed at the border of LADs **(C)**. Differentially expressed genes are in genomic regions that are not localized in LADs **(D)**. Gene Ontology (GO) analysis was performed for genes, which were either significantly up- or down-regulated compared to all genes (Fisher's Exact test followed by Benjamin Hochberg multiple test correction). Shown are the most significant categories **(E)**.

Figure 5. Transcription factor binding sites in differentially methylated regions.

Analysis of transcription factor binding sites was performed in DMRs and promoter regions of up-/down-regulated genes. The heatmap shows the -log10 *p*-value for motifs enriched in at least one DMR signature (Fisher's Exact test followed by Benjamin Hochberg multiple test correction, adj. *p*-value < 0.05) **(A)**. Motifs for the five most significant transcription factors are depicted **(B)**. Subsequently, binding sites in promoter regions of either up- or down-regulated genes was analyzed and motifs common in both lists are marked in bold (Fisher's Exact test followed by Benjamin Hochberg multiple test correction, adj. *p*-value < 0.05) **(C)**.

Figure 6. Scheme of chromosomal changes in replicative senescence.

Nuclear size increases; telomeres shorten and shift towards the nuclear center; DNA hypermethylation is rather observed in regions with the repressive histone mark H3K27me3, whereas hypomethylation is associated with H3K9me3 and LADs; gene expression changes are particularly observed in hypermethylated regions. DNAm changes and differentially expressed genes coincide with binding motifs for specific TFs.

Supplemental information

Supplemental table 1: EXCEL file of differentially expressed genes

Figure 1
Click here to download high resolution image

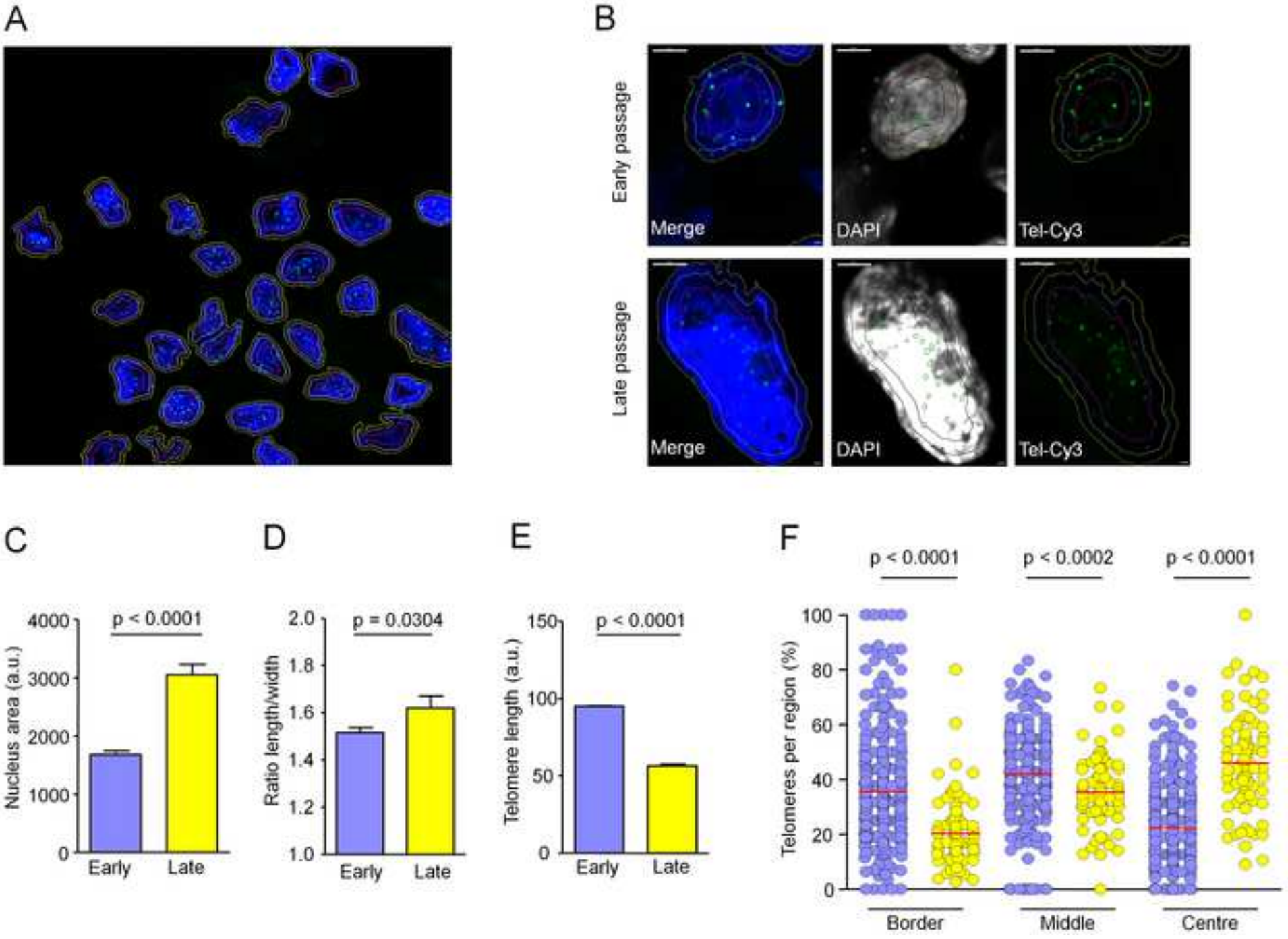

Figure 2
Click here to download high resolution image

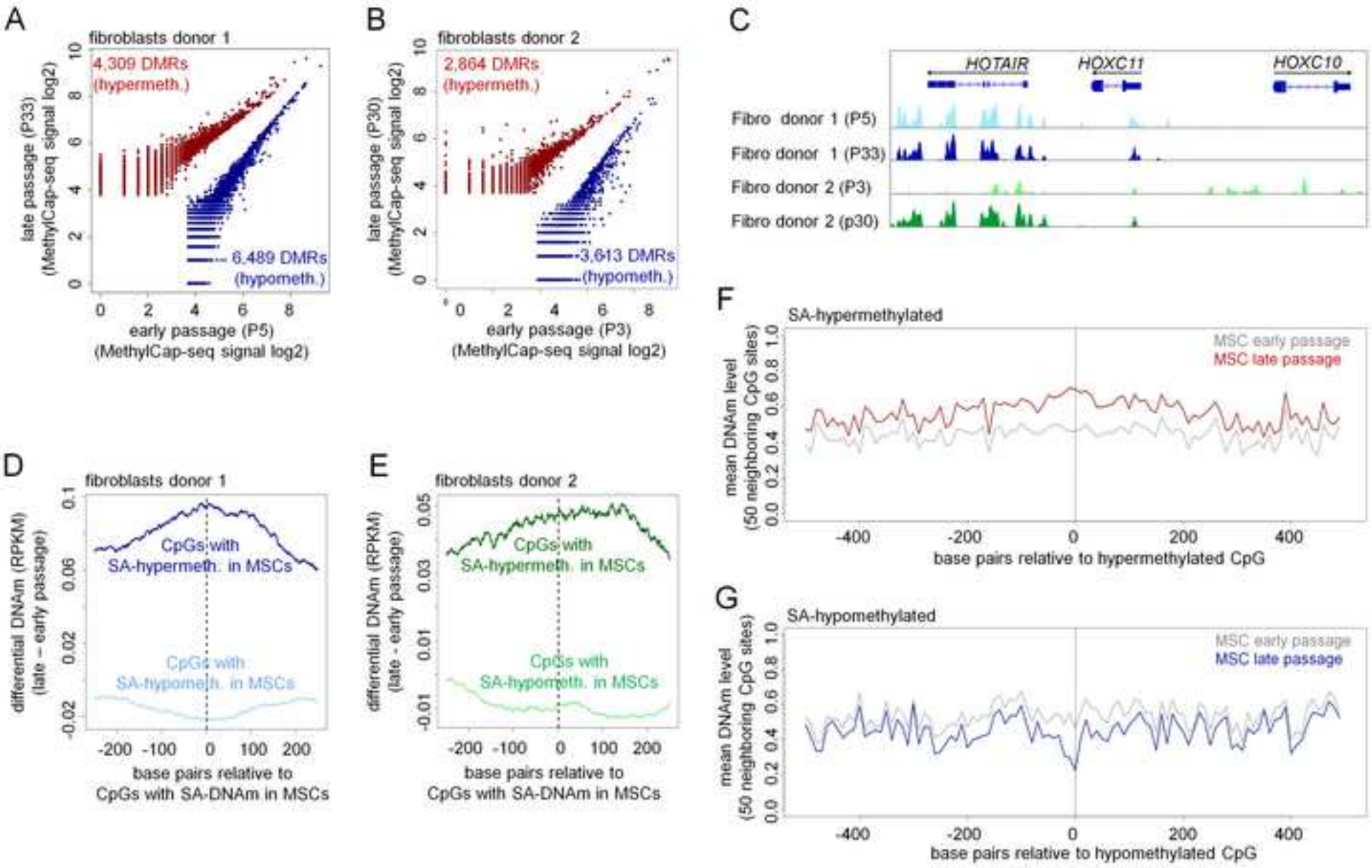

Figure 3
Click here to download high resolution image

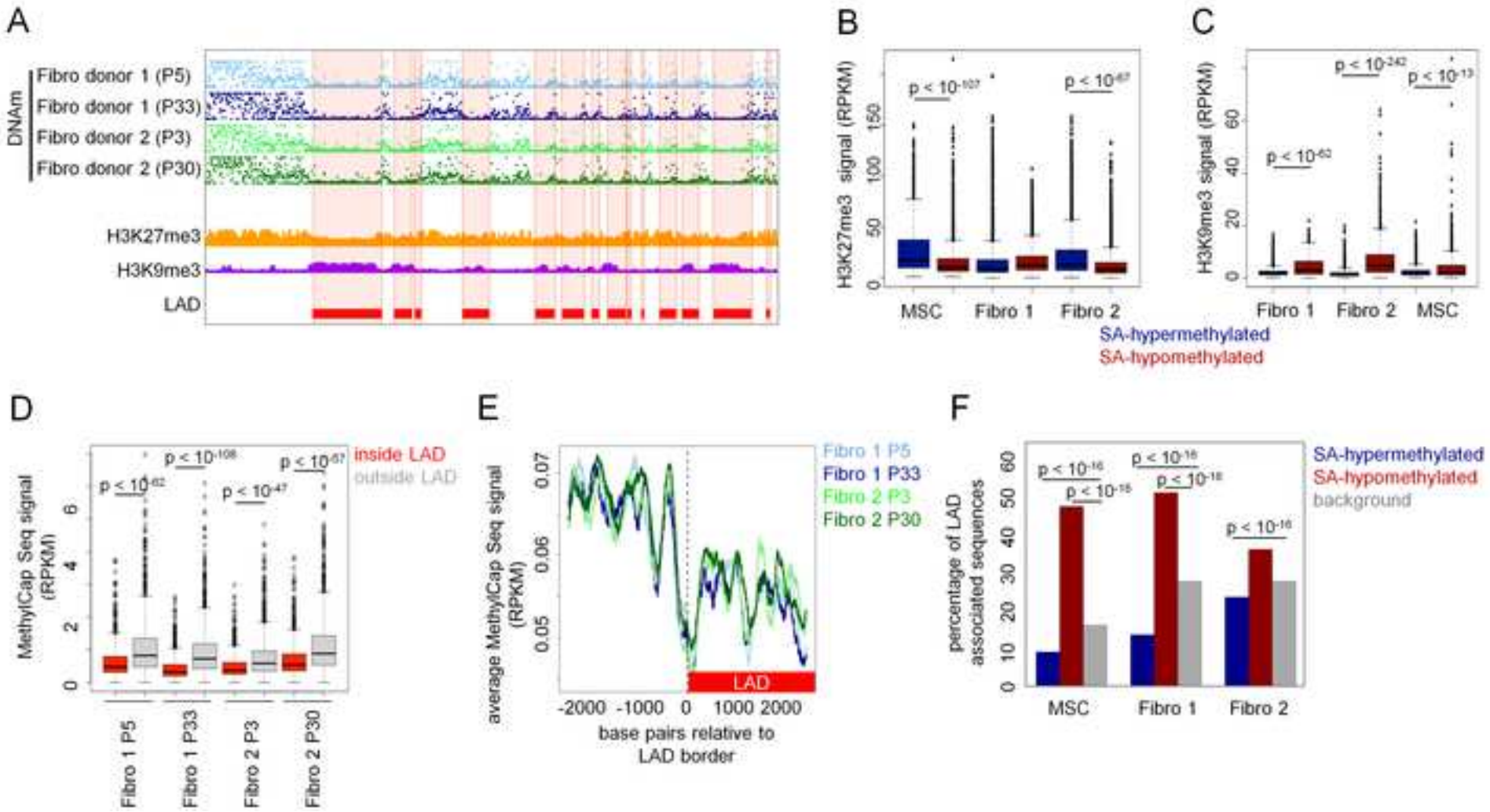

Figure 4

Click here to download high resolution image

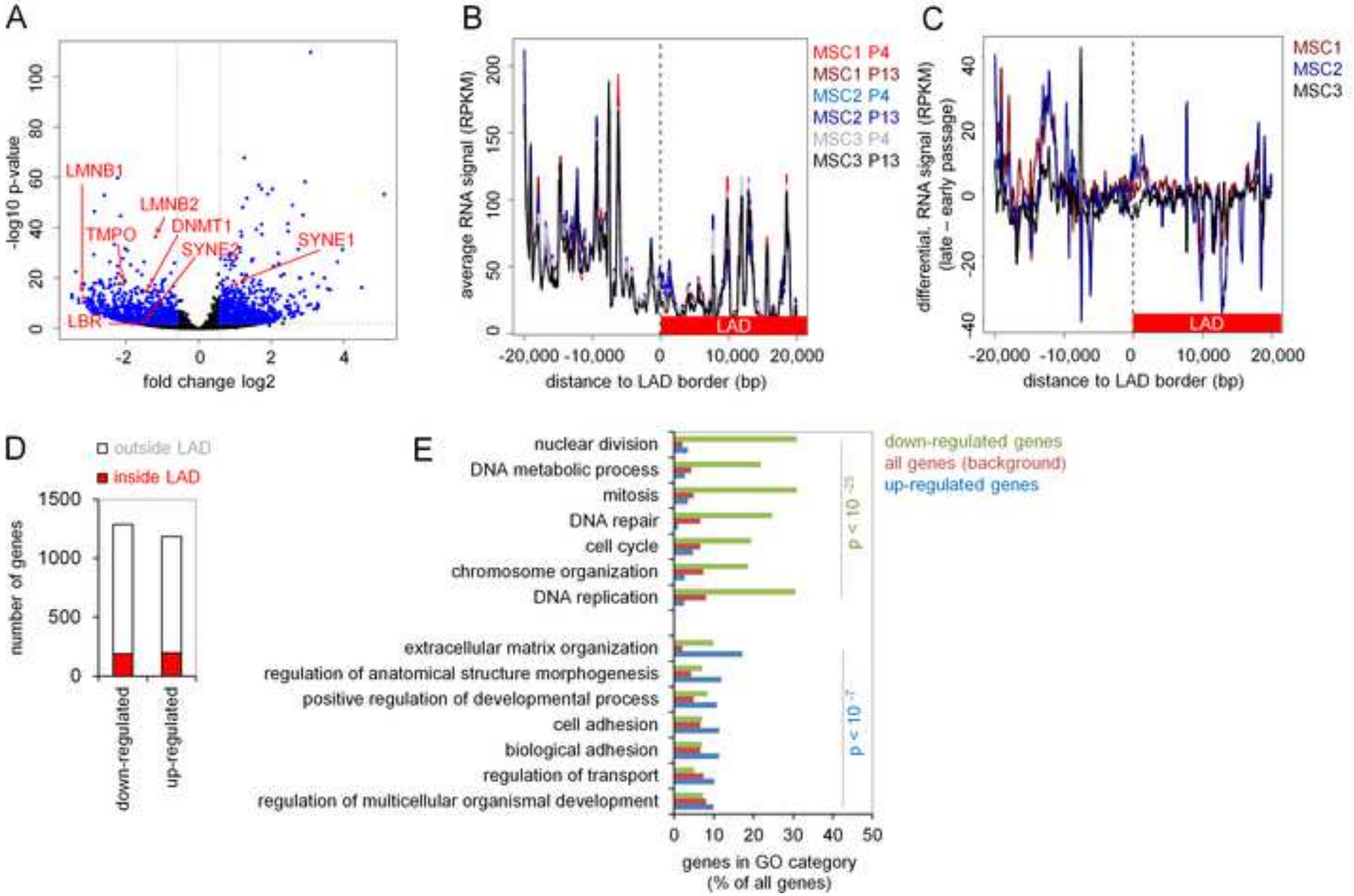

Figure 5
Click here to download high resolution image

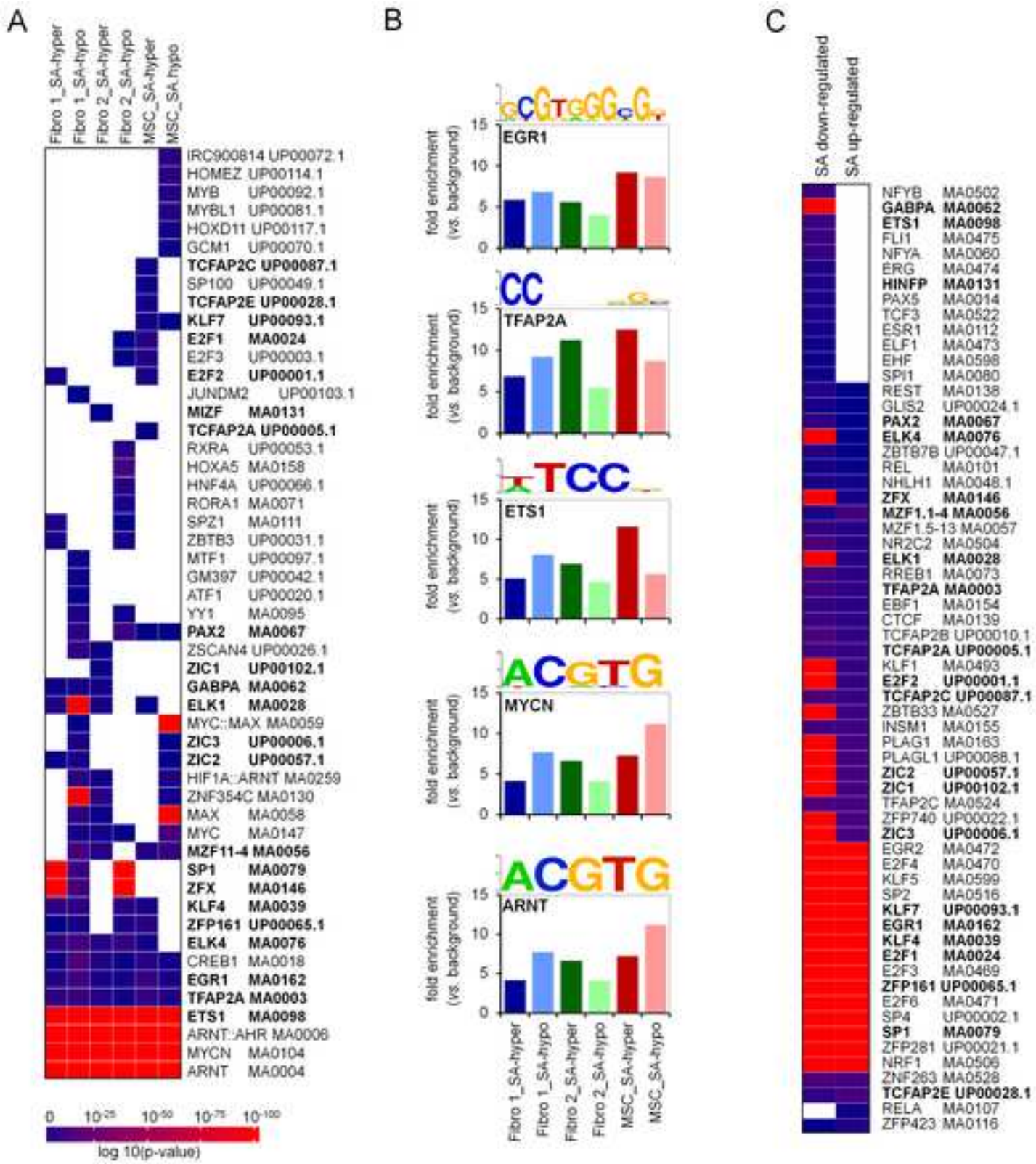

Figure 6
Click here to download high resolution image

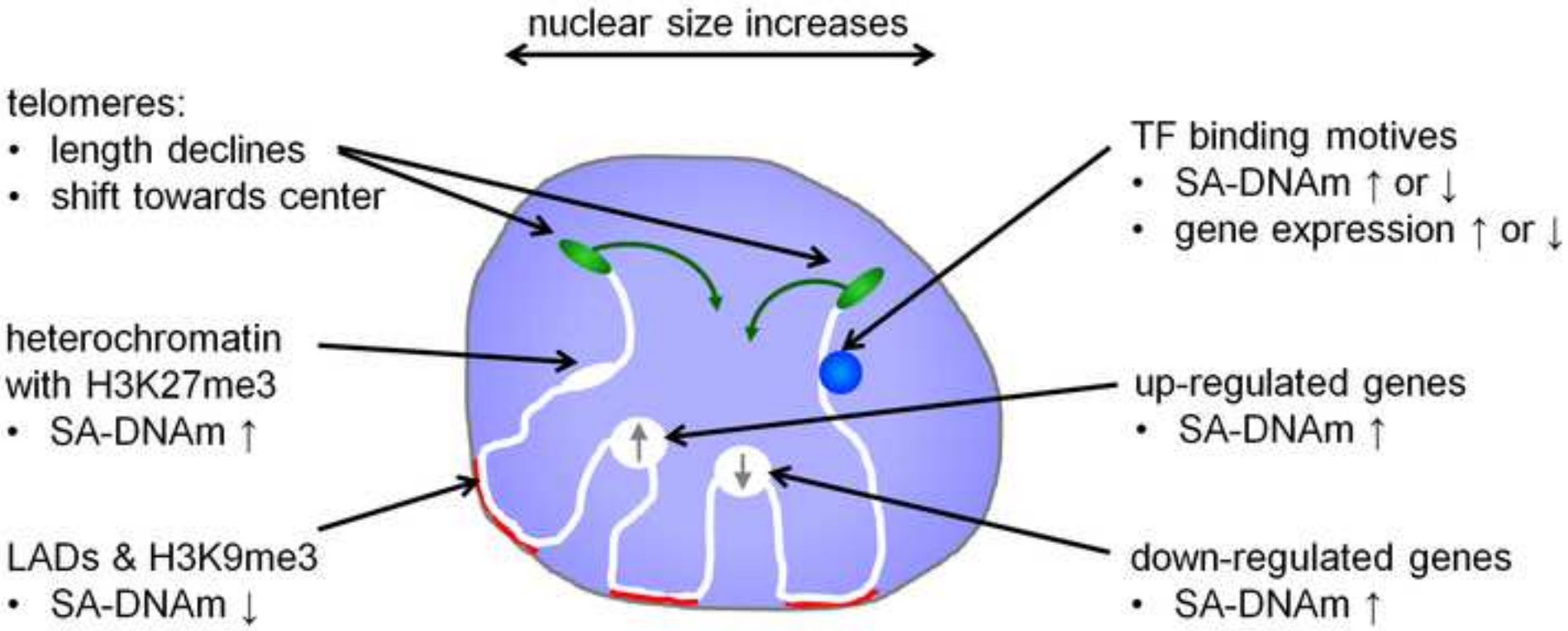

Supplemental Table S1

Click here to download Supporting Information: Differentially expressed genes 29.07.2014.xls